



Gold Nanoparticle Conjugated Organic Dye Nanocomposite Based Photostimulated Luminescent Enhancement and Its Application in Nanomedicine

Ketevan Chubinidze^{1,*}, Besarion Partsvania², Lali Devadze³, Tsisana Zurabishvili³, Nino Sepashvili³, Gia Petriashvili⁴, Mariam Chubinidze⁵

¹Department of Biology, I. Javakhishvili Tbilisi State University, Georgia

²Department of Biocybernetics, Institute of Cybernetics, Tbilisi, Georgia

³Department of Optical-Chemical Research, Institute of Cybernetics, Tbilisi, Georgia

⁴Department of Optically Anisotropic Systems, Institute of Cybernetics, Tbilisi, Georgia

⁵Faculty of Medicine, Tbilisi State Medical University, Tbilisi, Georgia

Email address:

Chubinidzeketino@yahoo.com (K. Chubinidze)

*Corresponding author

To cite this article:

Ketevan Chubinidze, Besarion Partsvania, Lali Devadze, Tsisana Zurabishvili, Nino Sepashvili, Gia Petriashvili, Mariam Chubinidze. Gold Nanoparticle Conjugated Organic Dye Nanocomposite Based Photostimulated Luminescent Enhancement and Its Application in Nanomedicine. *American Journal of Nano Research and Applications*. Special Issue: Nanotechnologies. Vol. 5, No. 3-1, 2017, pp. 42-47. doi: 10.11648/j.nano.s.2017050301.20

Received: February 3, 2017; **Accepted:** February 4, 2017; **Published:** February 28, 2017

Abstract: We have experimentally demonstrated that the emission of visible light from the polymer matrix doped with luminescent dye and gold nanoparticles (GNPs) can be enhanced with the use of surface plasmon coupling. GNPs can enhance the luminescence intensity of nearby luminescent dye because of the interactions between the dipole moments of the dye and the surface plasmon field of the GNPs. The electric charge on the GNPs and the distance between GNPs and luminescent dye molecules have a significant effect on the luminescence intensity, and this enhancement depends strongly upon the excitation wavelength of the pumping laser source. This ability of controlling luminescence can be beneficially used in developing contrast agents for highly sensitive and specific optical sensing and imaging. It opens new possibilities for plasmonic applications in nanobiology and nanomedicine. In particular, for example, luminescent dye-conjugated GNPs and gold nanorods (GNRs), can be used to target specific cancer cells, which is very important for the diagnosis and therapy of cancer.

Keywords: Luminescent Organic Dyes, Nanocomposite, Polymers, Gold Nanoparticles, Gold Nanorods, Near Infrared Spectrum, Nanomedicine

1. Introduction

The interaction of luminescent molecules with plasmons in metallic nanostructures and the physical phenomena related to nanoscale confinement of light have attracted the interest of physicists over recent years [1 – 3]. Fluorescence resonance energy transfer (FRET) is a nonradiative process when by an excited state donor transfers energy to a proximal ground state acceptor through long-range dipole–dipole interactions [4]. Metal nanoparticles (MNs) have created considerable interest in various fields of science and engineering because of their unique physical and chemical

properties, leading to potential applications in electronics, optical and magnetic devices [5, 6]. MNs can enhance the fluorescence of nearby fluorophores because the interactions between the dipole moments of the fluorophores and the surface plasmon field of the MNs [7 – 10]. Gold nanoparticles (GNPs) are among the most extensively studied nanomaterials. They are known to be the most stable metal nanoparticles [11, 12]. Numerous studies have been reported on the synthesis, property and application development of gold clusters, colloids, and nanoparticles [13 – 16]. In addition, combining the properties of GNPs with those of known organic dyes has already led to many interesting

applications including sensing of biologically relevant molecules [17, 18]. In this work we present GNPs formed and incorporated together with the luminescent dye Nile blue 690 perchlorate (NB 690) into a film of polyvinyl alcohol (PVA) and show the ability of the controlling luminescence enhancement that can be successfully used in nanomedicine. We have, therefore, chosen the PVA because of its ease of processability, solubility, mechanical and thermal stability. Light enhancement of a luminescent dye strongly depends on the factors that can be manipulated to obtain a desired luminescence: the distance between the luminescent dyes and the GNPs and the spectral overlap between the wavelength of pumping light source and GNPs plasmon resonance peak.

2. Sample Preparation

As the initial components we utilized next materials: macromonomer PVA with a number average molecular weight $M_w = 85,000 - 124,000$, 99+% hydrolyzed; colloidal monodispersed GNPs with 40 nm in size with concentration $7.15 \cdot 10^{10}$ N (nanoparticles) / ml and molecular weight 196.97 g / mol dispersed in an aqueous buffer (0.02 mg / ml); and glycerol solution 86 – 89% (T) with density 1.252 g / ml at 25°C. All components were purchased from Sigma–Aldrich. As the luminescent dye we used NB 690 (from “Exiton”). We made use these materials to prepare three separate mixtures. First, to obtain a polymer nanocomposite, an initial PVA was dissolved in colloidal monodispersed GNPs in 8 mg / 1 mL proportion, and then doped with 5% (w / w) glycerol solution and with 0.02 wt.% NB 690. After that to prepare second solution, PVA was dissolved in distilled water in the same concentration ratio as was done in case of colloidal monodispersed GNPs, i.e., in 8 mg / ml and was doped with 5% (w / w) glycerol solution and with 0.02 wt.% NB 690. The final mixture prepared consists of PVA incorporated GNPs. All mixtures were stirred for at least 3 h at room temperature to avoid an aggregation and obtain homogeneous solutions. Then the resulting solutions were deposited by drop coating to the glass surfaces treated with deionised water. The coated films on substrates were stored for 48 h at room temperature. After all procedures and solvent evacuation, films were detached from the glass substrates. Measured films thicknesses were about 50 μm .

3. Experimental

Absorbance and luminescence spectra of the samples were recorded by multi-fiber optic spectrometer (Avaspec–2048, “Avantes”). Photoexcitation of the nanocomposites were performed at $\lambda = 532$ nm, by using MSL–III–532 diode laser – 5 mW power (CNI, China). To determine a time resolved luminescence an Nd: YAG laser at $\lambda = 532$ nm coupled with Hamamatsu photomultiplier tube R374 and GHz digital oscilloscope (HP54110D) were utilized. The optical (“LOMO”), confocal scanning (“Leica”) and scanning electron microscope (SEM) were involved to investigate polymer nanocomposites at microscale. First, we have made a visual

comparison between two prepared polymer films. Using a spectrometer, the absorption spectrum for each sample was recorded. As shown in Figure 1, polymer film consisting of GNPs / NB 690 has less absorption than a polymer film doped just with NB 690. Besides, in the picture we show the absorption spectrum of PVA matrix doped with GNPs.

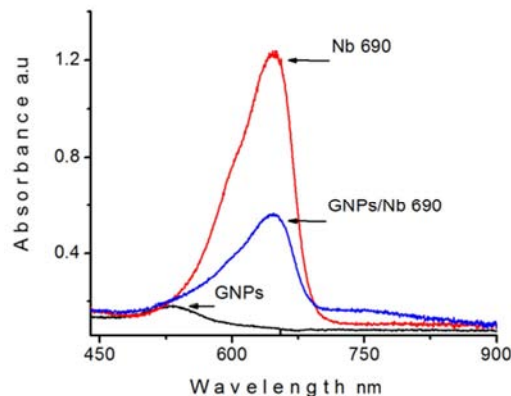


Figure 1. Absorption spectra of PVA doped with NB 690, GNPs / NB 690 and GNPs.

These differences in the transparency between PVA / GNPs / NB 690 and PVA / NB 690 can be explained with very strong interaction between GNPs and NB 690, which occurs due to the close proximity of GNPs and NB 690. Next we have studied if the fluorescence properties of NB 690 dyes were coupled to GNPs. In order to compare the intensities of the output lights from the PVA / GNPs / NB 690 and PVA / NB 690 composites, we recorded the luminescence spectra using a spectrometer. We note that under the experimental conditions, an excitation wavelength of 532 nm is far from the maximum of the absorption peak of NB 690 and coincides with the plasmon resonance peak of GNPs. As the result we obtained a strong enhancement of the luminescence when by the laser light was irradiated the nanocomposite PVA / GNPs / NB 690. Figure 2 displays the luminescence spectra emitted from PVA / NB 690 and PVA / GNPs / NB 690. It is obvious that the light intensity emitted from the nanocomposite PVA / GNPs / NB 690 is much stronger than the light intensity emitted from PVA / NB 690.

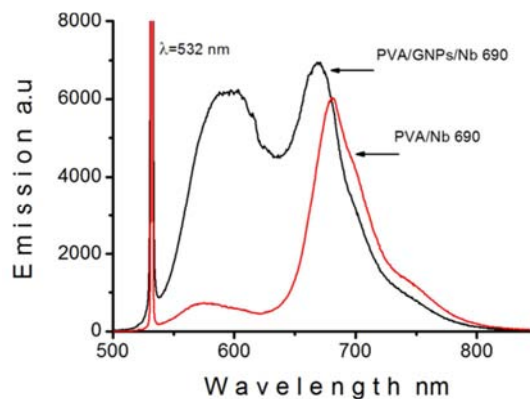


Figure 2. Induced light emissions from PVA / NB 690 and PVA / GNPs / NB 690 polymer composites pumped by laser with wavelength coincide to the absorption of GNPs.

4. Results and Discussions

In the description of the nature of the energy transfer from an organic luminescence dye to a GNP, a crucial role plays the distance dependence between the luminescence dye and the surface of a GNP. The altered electromagnetic field around the metal nanoparticle changes the properties of a dye that is placed in the vicinity. It can cause two enhancement effects: the first is an increase in the quantum efficiency of the dye and the second is an increase in the excitation rate of the dye. The induced collective electron oscillations associated with the surface plasmon resonance, give rise to induce local electric fields near the nanoparticle surface. Energy transfer from luminescent organic dyes to gold nanoparticles is generally considered to be the major process leading to the excited-state activation / deactivation of the dyes [19]. The most familiar mechanism is that of energy transfer via dipole–dipole interactions i.e. FRET, from an energy donor to an energy acceptor. The energy transfer efficiencies (E) have been measured using Equation (1) from the lifetime data,

$$E = 1 - \tau / \tau_0, \quad (1)$$

where τ and τ_0 are the lifetimes of the donor in the presence and absence of the acceptor, respectively. To determine a time resolved luminescence, the luminescence lifetimes of the samples were measured as a function of time after being excited by a beam of light. A pulsed Nd:YAG laser light of 5 ns with a wavelength of 532 nm was used to excite the PVP / NB 690 (to determine τ_0), and PVA / GNPs / NB 690 (to determine τ) composites. The detector used in this apparatus was a Hamamatsu photomultiplier tube R374 coupled to the GHz oscilloscope which displayed the decay of the luminescence intensity with respect to time. Estimated times were $\tau_0 \approx 8.24 \cdot 10^{-9}$ and $\tau \approx 1.36 \cdot 10^{-9}$ s, respectively. The induced electric field originating from the charge separation in the nanoparticle during the plasmon resonance oscillations is very large at very small distances from the surface. The dependence of the critical donor–acceptor distance (R_0) when energy transfer efficiency is 50%, on the spectral overlap for a particular donor–acceptor pair is expressed as:

$$R_0 = 0.211 (K^2 N^4 \Phi_D J(\lambda))^{1/6}, \quad (2)$$

where K^2 represents the relative orientation of the donor to the acceptor molecule, considering a random rotational diffusion for the small molecules, K^2 is taken to be 2/3 [20], N is the refractive index of the medium (1.4 for PVA / NB 690 / GNPs), Φ_D is the quantum yield of the donor in the absence of the acceptor, taken as 0.31, and $J(\lambda)$ is the overlap integral, which can be calculated from the numerical integration method using the following relation:

$$J(\lambda) = \frac{\int_0^\infty d\lambda \lambda^4 F(\lambda) \varepsilon_A(\lambda)}{\int_0^\infty d\lambda F(\lambda)}, \quad (3)$$

where $F(\lambda)$ is the luminescence intensity of the donor in the

wavelength range from λ to $(\lambda + \Delta\lambda)$ with the total intensity normalized to unity, $\varepsilon_A(\lambda)$ is the molar extinction coefficient of the acceptor. For GNPs with 40 nm size the molar extinction coefficient is equal to $8.42 \cdot 10^9 \text{ M}^{-1} \text{ cm}^{-1}$ (from Sigma–Aldrich). The fact that gold nanoparticles have very large molar extinction coefficients makes them potentially excellent energy acceptors according to Equation (2). The overlap integrals $J(\lambda)$ for the present donor–acceptor (GNPs / NB 690) were estimated to be $\approx 2.5 \cdot 10^{-6} \text{ M}^{-1} \text{ cm}^3$. The energy transfer efficiencies in Equation (1) can be rewritten as:

$$E = R_0^6 / (R_0^6 + r^6). \quad (4)$$

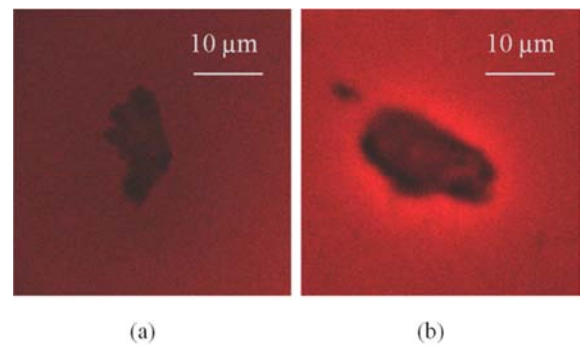


Figure 3. Images of PVA / NB 690 (a) and PVA / NB 690 / GNPs (b) composites, taken with confocal microscope.

According to the measured data for the energy transfer efficiencies from the Equation (1) we found $E = 0.84$. Finally, based on the experimental results and calculated data from the Equations (1 – 4), we found the distance between the dye molecules and GNPs, which are statistically distributed in the polymer medium, is equal 0.5 ± 0.15 nm. To visualize the distribution of GNPs / NB 690 pairs in PVA matrix we used polarized light microscope and confocal microscope. GNPs / NB 690 pairs that are homogeneously distributed in the PVA matrix are responsible for the enhancement of the background brightness. To show a difference in brightness between PVA / GNPs / NB 690 and PVA / NB 690 composites, we used a confocal microscope and excited the samples with adjusted light beam with the same wavelength intensities and the exposure times. As it is seen in Figure 3, the PVA / GNPs / NB 690 composite looks brighter than PVA / NB 690 composite.

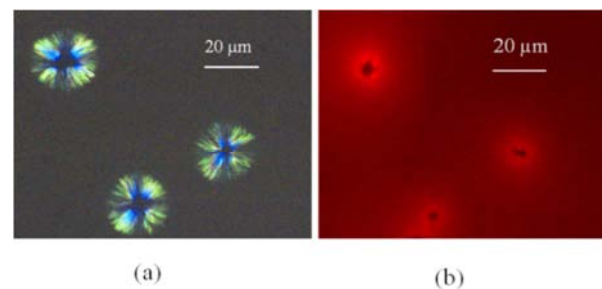


Figure 4. Images of GNPs / NB 690 clusters under optical (a) and confocal (b) microscopes.

Besides, we found that some amount of GNPs / NB 690

are prone to aggregate and form the clusters, which are the condensed quantity of GNPs and NB 690. The vivid “halos” surrounding the clusters demonstrate the enhancement of

light brightness which confirms the strong FRET effect between GNPs and NB 690, Figure 4.

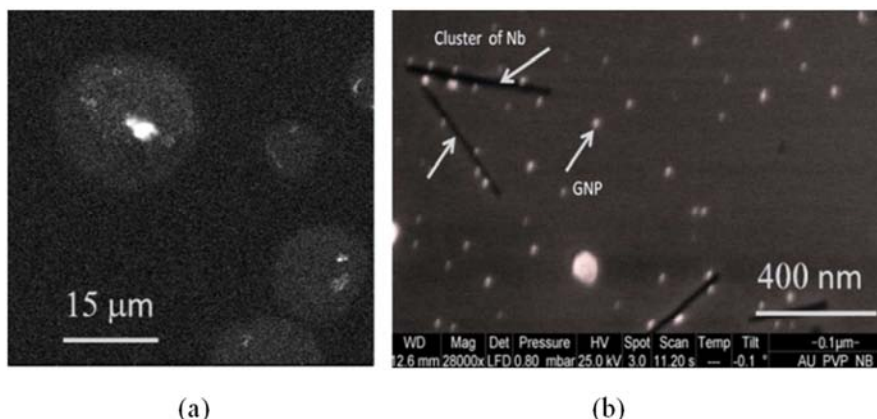


Figure 5. SEM images of GNPs / NB 690 polymer nanocomposite with low (a) and high (b) magnification.

By using of SEM, we have confirmed that GNPs are prone to aggregate along to NB 690 clusters. In Figure 5, the black stripes are the clusters of NB 690, whereas, white dots correspond to the GNPs.

5. Application of GNPs / GNRs / Luminescent Dye Probes as the Biomarkers

As the next step of our experiments, we have demonstrated that the obtained results can be suggested as a useful modality for the in-vitro representation of nanoparticle mediated cancer biomarkers, for the cell labeling and tracking in biological tissues through the luminescence. For this reason we used the two main types of GNPs, spherical and rode-like, to design the probes and demonstrate the light enhancement in the visible and near infrared (NIR) ranges of the optical spectrum. To show the luminescent enhancement in the visible part, we used two pieces of lungfish tissue inserted in the two dishes: one was filled with NB 690 luminescent dye, dissolved in double distilled water with the concentration $2 \cdot 10^{-5}$ g NB 690: 1.5 ml water, and the other one, filled with $2 \cdot 10^{-5}$ g NB 690: 1.5 ml water: $7.15 \cdot 10^{10}$ N GNPs / ml, dispersed in an aqueous buffer (0.02 mg / ml). Dishes were stored in a humidified atmosphere at 37°C, for 24 h in order to achieve a desired incubation rate of NB 690 and NB 90 / GNPs composites on the tissues. After the treatment by NB 690 and GNPs, tissues were washed two times with 1.5 ml Dulbecco Phosphate Buffered Saline. Then each solution was deposited by drop-coating to the glass slide treated with deionized water. The two coated films on substrate were stored for 24 h at room temperature to let the water evaporate completely. Obtained samples were examined and investigated using the optical and confocal microscopes. As shown in Figure 6, a light emission from tissue labeled with NB 690 / GNPs, Figure 6b, is much stronger, than that labeled just with NB 690 / luminescent

dye, Figure 6a.

GNRs functionalized with the fluorescent dyes offer a number of properties which make them suitable for use in biological applications, in particular, in the diagnosis of diseases such as cancer [21, 22]. In this work we have carried out the experiments for in-vitro demonstration of GNRs conjugated with NIR fluorescent dye complex, as an effective contrast agent for the visualization of prostate cancer cells. In this type of imaging, NIR dye / GNRs complex was introduced into the sample removed during the biopsy, Figure 7.

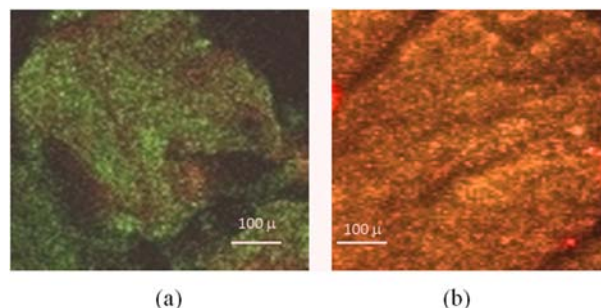


Figure 6. Labeled biological tissues with NB 690 (a), and GNP / NB 690 (b) composites.

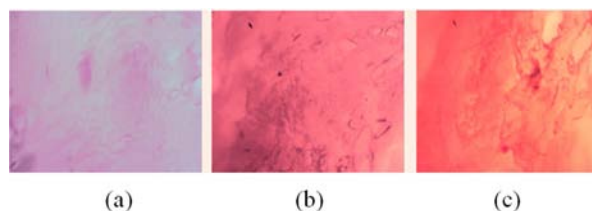


Figure 7. The microscopic images of tissue samples removed during a biopsy: (a) without NIR dye / GNR, (b) stained with NIR dye, and (c) labeled with NIR dye / GNRs.

Both substances, a NIR dye 3,3'-Diethylthiatricarbo cyanineiodide, and a GNR, with axial diameter 10 nm and longitudinal size 40 nm, were purchased from Sigma–Aldrich, Figure 8. Samples with GNRs / NIR dye / tissue

complex have been prepared similarly to the work conducted with spherical GNPs / NB 690 substances. Specimens were exposed by an external source of invisible NIR light that can deeply penetrate the biological tissue. When a light beam reaches the GNR / NIR dye complex, the dye emits a light which is then picked up by a CCD camera.

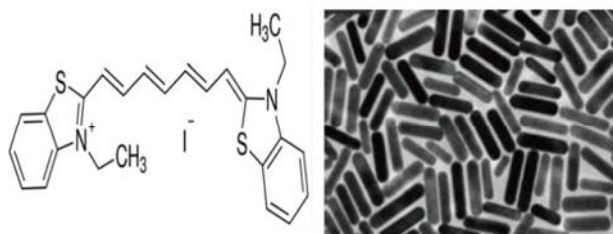


Figure 8. NIR dye 3,3'-Diethylthiatricocyanineiodide (a) and GNPs (b).

Thereby we have experimentally demonstrated that: (1) GNPs / NIR dye complex is prone to distribute across the location of the prostate cancer cells (suspected areas were predetermined by histo-morphological investigations); and (2) GNPs can dramatically enhance the light intensity of nearby fluorescent dye because of the interactions between the dipole moments of the fluorescent dye and the surface plasmon field of the GNPs, Figures 9 and 10.

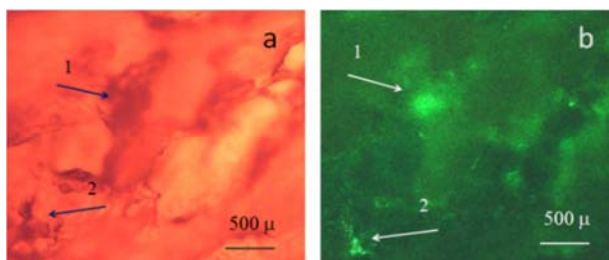


Figure 9. NIR dye / GNR doped cancer tissues as they look under the optical (a) and confocal (b) microscopes, equipped with CCD camera.

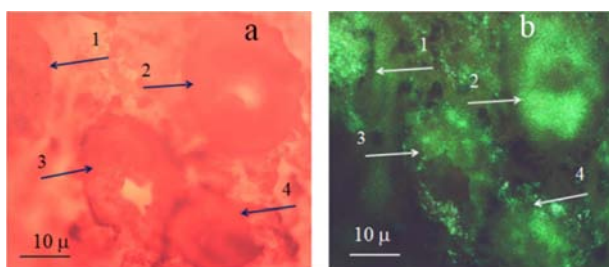
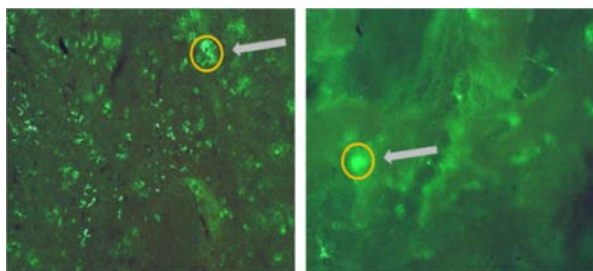
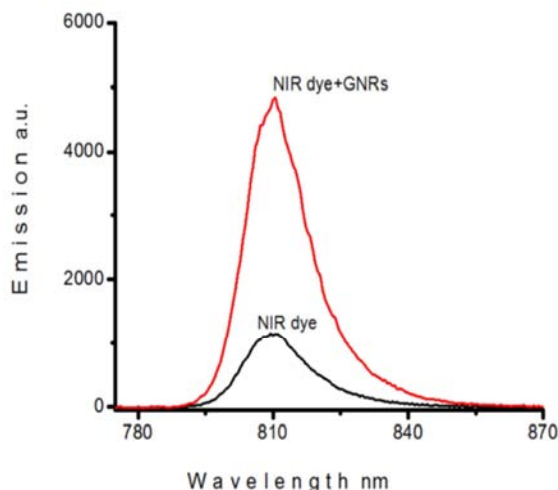


Figure 10. NIR dye / GNR doped cancer cells as they look under the optical (a) and fluorescent (b) microscopes, equipped with CCD camera.



(a)



(b)

Figure 11. Demonstration of the enhancement of luminescent intensity stimulated by GNPs using fluorescent microscope (a) and spectrometer (b).

Similarly to the experiments, carried out with GNPs conjugated organic dye nanocomposite, we have found that the electric charge on the GNPs and the distance between GNPs and NIR dye molecules have a significant effect on the luminescence intensity, and this enhancement depends strongly upon the excitation wavelength of the pumping laser source, Figure 11 (a and b). Herein, we note that the obtained results accomplished with prostate cancer cells visualization, are preliminary, and currently, we are going to conduct a number of experiments to confirm and evaluate the achieved outcomes.

6. Conclusions

We present here GNPs formed and incorporated together with luminescent dye NB 690 into a film of PVA. The increase of luminescence of the NB 690 results from its interaction with GNPs surface plasmons. The electric charge on GNPs, distance between them and luminescent dye molecules has a significant effect on the luminescence intensity, and this enhancement depends strongly upon the wavelength of the incident light. Based on the obtained results, we have demonstrated that GNPs conjugated with luminescent dyes can be considered as a useful modality for in-vitro representation of nanoparticle mediated cancer biomarkers, for the cell labeling and tracking in biological tissues through the luminescence. Besides, the GNPs, that have significant absorption in the tissue optical window, are the promising sensing and can change their scattering and absorption properties dramatically. Specificity of effect and selective targeting can be achieved, generally by functionalization of the GNPs with an NIR organic luminescent dye. This method can be highly advantageous for the early stage cancer detection and visualization, because the reduced scattering and absorption of NIR irradiation, which results in a deep penetration of light in the biological tissues.

References

- [1] T. D. Neal, K. Okamoto, and A. Scherer, "Surface plasmon enhanced emission from dye doped polymer layers," *Opt. Expr.*, vol. 13, pp. 5522-5527, 2005.
- [2] W. L. Barnes, A. Dereux, and T. W. Ebbesen, "Surface plasmon subwavelength optics," *Nature*, vol. 424, pp. 824-830, 2003.
- [3] A. Bouhelier and G. P. Wiederrecht, "Excitation of broad band surface plasmon polaritons: Plasmonic continuum spectroscopy," *Phys. Rev. B*, vol. 71, no. 195406, 2005.
- [4] K. E. Sapsford, L. Berti, and I. L. Medintz, "Materials for fluorescence resonance energy transfer analysis: Beyond traditional donor-acceptor combinations," *Angew. Chem. Int. Ed.*, vol. 45, pp. 4562-4589, 2006.
- [5] S. Eustis and M. A. El-Sayed, "Why gold nanoparticles are more precious than pretty gold: Noble metal surface plasmon resonance and its enhancement of the Radiative and nonradiative properties of nanocrystals of different shapes," *Chem. Soc. Rev.*, vol. 35, pp. 209-217, 2006.
- [6] R. Reisfeld, M. Eyal, and D. Brusilovsky, "Luminescence enhancement of Rhodamine 6G in sol-gel films containing silver aggregates," *Chem. Phys. Lett.*, vol. 153, pp. 210-214, 1988.
- [7] K. Aslan, I. Gryczynski, J. Malicka, E. Matveeva, J. R. Lakowicz, and C. D. Geddes, "Metal-enhanced fluorescence from plastic substrates: An emerging tool in biotechnology," *Curr. Open Biotechnol.*, vol. 16, pp. 55-62, 2005.
- [8] J. R. Lakowicz, "Radiative decay engineering: 5. Metal-enhanced fluorescence and plasmon emission," *Anal. Biochem.*, vol. 337, pp. 171-194, 2005.
- [9] W. Zhong, "Nanomaterials in fluorescence-based biosensing," *Anal. Bioanal. Chem.*, vol. 394, pp. 47-59, 2009.
- [10] M. Atlan, P. Desbiolles, M. Gross, and M. Coppey-Moisan, "Parallel heterodyne detection of dynamic light-scattering spectra from gold nanoparticles diffusing in viscous fluids," *Opt. Lett.*, vol. 35, pp. 787-789, 2010.
- [11] A. Borriello, P. Agoretti, A. Cassinese, P. D'Angelo, G. T. Mohanraj, and L. Sanguigno, "Electrical bistability in conductive hybrid composites of doped polyaniline nanofibers-gold nanoparticles capped with dodecane thiol," *J. Nanosci. Nanotechnol.*, vol. 9, pp. 6307-6314, 2009.
- [12] C.-W. Hu, Y. Huang, and R. C.-C. Tsiang, "Thermal and spectroscopic properties of polystyrene / gold nanocomposite containing well-dispersed gold nanoparticles," *J. Nanosci. Nanotechnol.*, vol. 9, pp. 3084-3091, 2009.
- [13] M.-C. Daniel and D. Astruc, "Gold nanoparticles: Assembly, supramolecular chemistry, quantum-size-related properties, and applications toward biology, catalysis, and nanotechnology," *Chem. Rev.*, vol. 104, pp. 293-346, 2002.
- [14] C. Burda, X. Chen, R. Narayanan, and M. A. El-Sayed, "Chemistry and properties of nanocrystals of different shapes," *Chem. Rev.*, vol. 105, pp. 1025-1102, 2005.
- [15] E. Katz and I. Willner, "Integrated nanoparticle-bio-molecule hybrid systems: Synthesis, properties, and applications," *Angew. Chem. Int. Ed.*, vol. 43, pp. 6042-6108, 2004.
- [16] M. J. Kogan, N. G. Bastus, R. Amigo, D. Grillo-Bosch, E. Araya, E. Araya, A. Turiel, A. Labarta, E. Giral, and V. F. Puentes, "Nanoparticle-mediated local and remote manipulation of protein aggregation," *Nano Lett.*, vol. 6, pp. 110-115, 2006.
- [17] L. Shang, Ch. Qin, T. Wang, M. Wang, L. Wang, and Sh. Dong, "Fluorescent conjugated polymer-stabilized gold nanoparticles for sensitive and selective detection of cysteine," *J. Phys. Chem. C*, vol. 111, pp. 13414-13417, 2007.
- [18] J. Griffin, A. K. Singh, D. Senapati, P. Rhodes, K. Mitchell, B. Robinson, E. Yu, and P. Ch. Ray, "Size-and distance-dependent nanoparticle surface-energy transfer (NSET) method for selective sensing of hepatitis C virus RNA," *Chem. Eur. J.*, vol. 15, pp. 342-351, 2009.
- [19] K. G. Thomas and P. V. Kamat, "Chromophore functionalized gold nanoparticles. Review Article," *Acc. Chem. Res.*, vol. 36, pp. 888-898, 2003.
- [20] J. R. Lakowicz, "Principles of Fluorescence Spectroscopy, 3rd Ed.," New York: Springer, 938 pp., 2006.
- [21] P. J. Cassidy, G. K. Radda, "Molecular imaging perspectives," *J. Royal Soc. Interface*, vol. 2, pp. 133-144, 2005.
- [22] K. McLarty and R. M. Reilly, "Molecular imaging as a tool for personalized and targeted anticancer therapy," *Clin. Pharmacol. Ther.*, vol. 81, pp. 420-424, 2007.